Evolution in the Clustering of Galaxies to $r = 26$

Tereasa G. Brainerd[1], Ian Smail[2], and Jeremy Mould[3]

[1]Theoretical Astrophysics, Caltech 130-33, Pasadena, CA 91125, USA
[2]Palomar Observatory, Caltech 105-24, Pasadena CA 91125, USA
[3]Mount Stromlo and Siding Springs Observatories, Private Bag, Weston P.O., ACT 2611, Australia

ABSTRACT

We present results for the two-point angular correlation function of galaxies, $\omega(\theta)$, to a limiting magnitude of $r = 26$. Our catalogue is constructed from deep imaging using the COSMIC imaging spectrograph on the Hale 5-m. The final sample is 97% complete to $r = 26.0$ yielding ∼5700 galaxies over a 90.1 sq. arcmin field. Our analysis shows $\omega(\theta)$ for faint galaxies can be parameterised by a power law of the form $A_\omega\theta^{-0.8}$, in agreement with the angular clustering statistics of shallower catalogues. The derived amplitude, A_ω, for our catalogue is small, but non-zero. We combine this measurement with the latest statistical constraints on faint galaxy redshifts from gravitational lensing studies, which imply that the bulk of the $r \lesssim 26$ field galaxies should be at redshifts $z \sim 1$. We show that our derived A_ω is significantly lower than that predicted from the local bright, optically-selected galaxy correlation function using the lensing-determined galaxy redshift distribution and modest growth of clustering. However, this simplistic model does not include the variation in observed morphological mix as a function of redshift and apparent magnitude in our sample. At our faintest limits we reach sufficiently high redshifts that differential K-corrections will result in the observed galaxy mix being dominated by star bursting dwarf and low surface brightness irregulars, rather than the early-type systems used to define the local bright galaxy correlation function. Adopting the correlation function measured locally for these low surface brightness galaxies and assuming modest clustering evolution, we obtain reasonable agreement between our model and observations. This model, therefore, supports the scenario in which the high number density of faint galaxies is produced by normally clustered star forming dwarf galaxies at modest redshifts.

Key words: galaxies: clustering – galaxies: evolution – cosmology: observations – large-scale structure of the Universe

1 INTRODUCTION

The observed surface density of faint galaxies far exceeds the number predicted from a simple extrapolation of the local universe (the no evolution model; NE), irrespective of the cosmological geometry. However, to the faintest limits measurable the distribution of galaxies in redshift is a close match to that predicted by the NE model. Since at fainter limits galaxies become progressively bluer, the 'excess' population is primarily caused by an increase in the space density of blue low-luminosity galaxies at modest redshifts. The exact nature of this blue excess population is currently one of the major questions in observational cosmology and has significant impact on our understanding of galaxy formation and evolution.

Observationally, one of the cheapest statistics to obtain for samples of faint galaxies is the

strength of their clustering as seen in projection on the plane of the sky. This is commonly measured using the two-point angular correlation function, $\omega(\theta)$, defined by

$$dP = n^2[1 + \omega(\theta)]d\Omega_1 d\Omega_2, \tag{1}$$

where n is the mean number density of galaxies and dP is the probability in excess of Poisson of observing a pair of galaxies in solid angle elements $d\Omega_1$ and $d\Omega_2$ that are separated by an angle θ on the sky. To a given depth, $\omega(\theta)$ is dependent upon the redshift distribution of the sources, $N(z)$, and their 3-dimensional real space clustering strength, $\xi(r, z)$. Thus $\omega(\theta)$ is a sensitive test of both the luminosity and clustering evolution of faint galaxies (Koo & Szalay 1984). This fact, combined with the advent of efficient large format CCD detectors, has led to a recent flurry of interest in using the correlation strength of faint galaxies to study their nature (Neuschaefer, Windhorst & Dressler 1991; Efstathiou *et al.* 1991; Couch, Jurcevic & Boyle 1993; Roche *et al.* 1993).

At the bright magnitudes accessible with plate material from Schmidt telescopes ($B \lesssim 20$), $\omega(\theta)$ has been shown to follow a power law form: $\omega(\theta) = A_\omega \theta^{-\delta}$ with $\delta \approx 0.8$ (Groth & Peebles 1977; Shanks *et al.* 1980; Maddox *et al.* 1990). The value of A_ω depends upon the depth of the survey, but the derived values are in reasonable agreement when the results from different catalogues are rescaled to similar depths. Using plates from 4-m class telescopes it is possible to go somewhat fainter ($B \lesssim 24$), while still covering a large area. The studies at this depth are in less agreement, but do seem to support a continued $\delta \approx 0.8$ exponent for $\omega(\theta)$ to at least $B \sim 23$ (Koo & Szalay 1984; Stevenson *et al.* 1985 (SSFM)).

To reach still fainter limits CCDs have to be employed, with a resulting large reduction in sky coverage. As mentioned, several groups have attempted to measure $\omega(\theta)$ using CCD imaging and we briefly summarise these studies. Neuschaefer, Windhorst & Dressler (NWD, 1991) used g imaging over a 720 sq. arcmin area complete to $g \sim 24.5$ (roughly $R \sim 23.5$) and claim little change in the index, δ, of $\omega(\theta)$ from the value at brighter magnitudes. However, they do see a strong decline in the amplitude, A_ω, to $g \sim 24.5$. Efstathiou *et al.* (EBKTG, 1991) used multi-colour data on a number of small fields (each about 10 sq. arcmin) to measure $\omega(\theta)$ to $B < 26$ or $R < 25$. Their sample shows very weak clustering at their faintest limits and from this they conclude that a large fraction of the faint galaxies in their sample belong to a weakly clustered population which is not seen today. By far the largest study is that of Couch, Jurcevic & Boyle (CSB, 1993) who analysed a 4 sq. degree area to $R \lesssim 23$ and, as NWD, they found no change in δ with depth, while A_ω declined strongly. They conclude that their observations are inconsistent with linear growth in a standard CDM cosmogony. Finally, Roche *et al.* (RSMF, 1993) analysed a total of roughly 300 sq. arcmin in B and R, with the R sample limited at $R \leq 23.5$. Adopting a $\theta^{-0.8}$ power law for $\omega(\theta)$, they studied the variation of A_ω with depth and their analysis shows the, by now familiar, decline in A_ω at fainter magnitudes. They interpret their result as support for a model in which the faint galaxies have a clustering amplitude similar to local bright galaxies, but are distributed across a wide redshift range: $1 \lesssim z \lesssim 3$.

The recent study of Bernstein *et al.* (1994) used both plate material and statistical information on the redshift distribution of galaxies to $B \sim 22$ to estimate $\xi(r)$ on small scales at two different epochs: $z \sim 0.18$ and $z \sim 0.27$. Their results are significantly lower than predictions of models extrapolated from local bright galaxy clustering. However, their observations are consistent with the assumptions of modest clustering growth and that the bluest 60-70% of their sample have present-day clustering similar to IRAS-selected samples, which are intrinsically more weakly clustered than bright optically-selected samples (Saunders, Rowan-Robinson & Lawrence 1992, SRRL; Fisher *et al.* 1994).

A more direct approach to study the evolution of the two-point spatial correlation function, $\xi(r)$, uses the extensive field redshift samples which are gradually becoming available. From the large

Broadhurst, Ellis & Colless AAT redshift survey, Cole *et al.* (1994) analysed both the evolution in $\xi(r)$ and possible differences between the clustering of strongly and weakly star-forming galaxies (as indicated by their [OII] emission). They detected no evolution in $\xi(r)$ out to $z \sim 0.6$ and no significant difference between the clustering strengths of the [OII]-weak and [OII]-strong populations. However, at the limit of this study ($B \sim 22$) neither the apparent surface density of galaxies nor their clustering amplitude depart significantly from the NE prediction and, thus, the measurements are not particularly sensitive to any excess population.

The CCD studies of the angular correlation function of faint galaxies, while in broad agreement about the strong decline of the clustering strength of galaxies at fainter apparent magnitudes, differ in the interpretation of this result. Their inconclusive nature has partly arisen from our lack of information about the redshift distribution of very faint field galaxies. Most of the quantitative analyses undertaken adopt pure-luminosity evolution models to describe $N(z)$ for the faint galaxy samples. These models, even in their milder forms, are in conflict with the observed redshift distribution in faint field surveys (e.g. Glazebrook *et al.* 1994) and their applicability at even fainter magnitudes must, therefore, be in doubt. At the depths probed by the current samples use to estimate $\omega(\theta)$, it is likely that even 10-m class telescopes will be unable to provide complete spectroscopic samples. Nevertheless, some distance information is available for these very faint sources.

Firstly, spectroscopic redshifts have been measured for a small, but growing, sample of giant gravitationally lensed arcs. These arcs are highly distorted images of serendipitously placed galaxies seen through the cores of rich, moderate redshift clusters. They should, therefore, represent an unbiased sample of high-redshift faint field galaxies. This has been confirmed by Smail *et al.* (1993), who determined optical and optical-infrared colours of arcs and found that the colours were representative of the bulk of the faint field population. The current sample of giant arcs has a modest median redshift of $\langle z \rangle \sim 1$ with intrinsic source magnitudes of $B \sim 25$–26.

Statistical information is available on the distances of samples much larger than that of the giant arcs from analyses of weak lensing by rich clusters of galaxies (Smail *et al.* 1994; Kneib *et al.* 1994). Both of these studies indicate that the bulk of the $B \sim 26$–27 population lies at redshifts $z \sim 1$. In particular, the analysis of an I selected sample by Smail *et al.* (1994) gives a preferred redshift distribution peaked around $\langle z \rangle \sim 0.8$, similar to the distribution of the giant arc sample. The general shape of the redshift distributions indicated by the various lensing analyses are close to their respective NE model predictions. While the NE model is physically implausible at the distances and, hence, look-back times probed at these faint limits, the form of the predicted distribution is similar to that expected from the Burst model of Broadhurst, Ellis & Shanks (1988) (see also Babul & Rees 1992). This model effectively steepens the faint end slope at moderate redshifts by invoking short periods of intense star formation in intrinsically faint galaxies[1] to boost the faint number counts, while retaining the general form of the NE redshift distribution (see also McGaugh 1994). The faint counts are thus dominated by a population of blue, star-forming dwarf galaxies at modest redshifts. We therefore adopt the form of the NE redshift distribution as the $N(z)$ for our standard model in the analysis below.

Another currently fashionable galaxy evolution model, which predicts an $N(z)$ for the faint field population close to that observed, is the Merger model of Broadhurst, Ellis & Glazebrook (1992). Unfortunately, the clustering evolution of the merging galaxy population in this model is likely to be complex and little theoretical work has been done on predicting this evolution. We will therefore not compare our observations with this model in the discussion below.

RSMF claim that at their very faintest limits ($B \sim 25$) $\omega(\theta)$ reaches a lower limit and then

[1]In the discussion that follows we will use the term 'dwarf' for these intrinsically low-luminosity and low surface brightness (LSB) galaxies; this is used with no implication for the morphological nature of the systems.

flattens out. Such a flattening, if it is confirmed, might indicate the presence of a high-redshift cut-off in the distributions of faint galaxies, either due to galaxy formation or the Lyman limit entering the bandpass for high-redshift sources. The existence of such a large population of high-redshift galaxies would not be consistent with the lensing-derived $N(z)$. The simplest method to distinguish between these possibilities is to repeat this measurement in a redder passband. Therefore, we have undertaken a study of the evolution of the clustering strength of galaxies in a sample of faint galaxies selected in a red passband (Gunn r) to an effective magnitude limit deeper than all previous studies ($r \sim 26$). By combining these observations with the latest constraints on the distance to the faint galaxy population from lensing studies, we hope to gain new insight into the clustering evolution of distant galaxies. Our dataset also differs from those used previously in that it has both good seeing and high spatial sampling, resulting in negligible confusion at our faintest limits.

2 OBSERVATIONS

The observations analysed here were originally taken to select targets for a deep spectroscopic survey with the 10-m Keck-I telescope. The data have also been used to study the coherent distortion of faint galaxy images resulting from weak gravitational lensing by large-scale structure (Mould *et al.* 1994). The dataset and its reduction to a catalogue of detected objects is detailed in Mould *et al.* (1994) and here we present only a brief outline.

The final dataset consists of a total of 24.0 ksec integration in Gunn r and 6.0 ksec in Gunn g on a single blank field. This was all taken under good conditions (seeing 0.7–0.9 arcsec) with the COSMIC imaging spectrograph on the 5-m Hale telescope. In direct imaging mode, COSMIC has a 9.5×9.5 arcmin field with 0.28 arcsec/pixel sampling. The final stacked r image has a 1σ surface brightness limit of $\mu_r = 28.8$ mag arcsec^{-2}, seeing of 0.87 arcsec FWHM, and a total area of 90.1 sq. arcmin. The object catalogue created from this frame using the FOCAS image analysis package (Valdes 1982) contains ∼6600 objects brighter than the 80% completeness limit of $r = 26.2$. Adopting an extremely conservative magnitude limit of $r \leq 26.0$, where the detections are roughly 97% complete, we obtain a cumulative surface density of 71.8 galaxies per sq. arcmin (5–7 times the NE prediction, depending upon Ω_0). To calculate the equivalent R limit we use the typical galaxy colour at this depth and the photometric conversion of Kent (1985) giving $R \sim r - 0.55$ and a limit of $R \lesssim 25.5$. The g-band data are deep enough to provide $g-r$ colours accurate to $\Delta(g-r) \sim 0.2$ at this limit. Our magnitude definition follows that of Lilly *et al.* (1991), adopting isophotal magnitudes until an object's isophotal diameter shrinks below 3 arcsec, at which point photometry within a fixed 3 arcsec aperture is used. The catalogue of galaxies with $r \leq 26.0$ is used as the basic data for the analysis detailed below.

A mask frame defining areas around bright objects and along the frame boundaries, where the efficiency of galaxy detection is lower than average, was also constructed. Approximately 5% of the total area of the frame is masked out and these regions are excluded in the analysis below.

3 ANALYSIS

3.1 Estimation of $\omega(\theta)$

We estimate $\omega(\theta)$ for the galaxies using the direct pair-counting method proposed by Landy & Szalay (1993),

$$\hat{\omega}(\theta) = \frac{DD - 2DR + RR}{RR}, \tag{2}$$

where DD, DR, and RR are the number of distinct data-data, data-random, and random-random pairs (appropriately scaled by the number of data and random points) in a given angular separation

bin. To estimate $\omega(\theta)$ we use 50,000 random points over the geometric area covered by the data catalogue, taking into account the regions which are masked out due to the presence of bright objects or the frame edge. The mean $\hat{\omega}(\theta)$ obtained from 50 independent sets of random points is computed for angular scales, $17'' \leq \theta \leq 427''$, valid for our dataset (0.14 to 3.5 Mpc at the median redshift of our adopted $N(z)$). Errors for $\hat{\omega}(\theta)$ are estimated using 50 bootstrap resamplings of the data (e.g. Barrow, Bhavsar, & Sonoda 1984).

As a consistency check of $\hat{\omega}(\theta)$ obtained using the direct estimator above, we have applied a counts-in-cells estimator

$$\hat{\omega}(\theta) = \frac{\langle N_i N_j \rangle}{\langle N_i \rangle \langle N_j \rangle} - 1, \tag{3}$$

where N_i and N_j are the number of galaxies found in cells i and j, and the brackets denote an average over pairs of cells separated by an angle $\theta \pm \delta\theta$. The galaxies were binned in $5'' \times 5''$ cells and $\hat{\omega}(\theta)$ computed using equation (3) above. Excellent agreement was found between the results of the direct and counts-in-cells estimators.

3.2 A_ω and the Integral Constraint

In the calculation of $\hat{\omega}(\theta)$ the observed number density of galaxies on the CCD frame (to a given magnitude limit) is used to estimate the true mean density of galaxies at that magnitude limit. The small area of the frame results in a bias in the estimate of $\omega(\theta)$ due to the well-known "integral constraint" which has the effect of reducing $\hat{\omega}(\theta)$ by an amount

$$C = \frac{1}{\Omega^2} \int \int \omega(\theta) d\Omega_1 d\Omega_2, \tag{4}$$

where the integrals are performed over the total solid angle, Ω, of the regions of the field not excluded by the detection mask.

Assuming a power law form for the two-point correlation function, $\omega(\theta) = A_\omega \theta^{-\delta}$ with $\delta = 0.8$, as suggested by previous brighter surveys, we find $C = 0.0146 A_\omega$ for our field geometry and galaxy detection mask.

In order to compare estimates of $\omega(\theta)$ from catalogues with differing depths, it is common to quote the value of $\hat{\omega}(\theta = 1^\circ)$ after adopting a power law form for $\hat{\omega}(\theta)$ with $\delta = 0.8$ and correcting A_ω for both the integral constraint and the dilution effect of faint stars which have not been removed from the object catalogues. The corrected amplitude is then

$$A_\omega^{\rm corr} = \left(\frac{N_{\rm obj}}{N_{\rm obj} - N_{\rm s}} \right)^2 A_\omega^{\rm IC}, \tag{5}$$

where $N_{\rm obj}$ is the total number of objects used in the determination of $\hat{\omega}(\theta)$, $N_{\rm s}$ is the number of contaminating stars (estimated from the model of Bahcall & Soneira 1980), and $A_\omega^{\rm IC}$ is the amplitude of the best-fit power law with $\delta = 0.8$, corrected for the integral constraint. Table 1 summarizes our results for these quantities, where the value of $A_\omega^{\rm corr}$ is appropriate for θ in units of arcseconds. The error on $A_\omega^{\rm corr}$ has been estimated from Monte Carlo simulations of fields populated with galaxies distributed with a known $\omega(\theta)$ of the form $A_\omega \theta^{-0.8}$. These simulated fields were constructed using the iterative tree method of Soneira & Peebles (1978). The resulting fractional error in A_ω rises from 10% for our brightest bin to 20% for the faintest. The stellar contamination correction from the Bahcall & Soneira (1980) model is highly uncertain; however, a factor of 2 increase the number of stars in our faintest bins amounts to only a 1 σ increase in A_ω.

3.3 Expected Correlations

From local bright, optically-selected galaxy surveys, the two-point spatial correlation function, $\xi(r)$, is well-approximated by a power law of the form $\xi(r) = (r/r_0)^{-\gamma}$, $\gamma \approx 1.8$ and $r_0 \approx 5.5h^{-1}$Mpc, for $10h^{-1}\text{kpc} \lesssim r \lesssim 10h^{-1}\text{Mpc}$ (h is the present value of the Hubble parameter in units of 100 kms sec^{-1} Mpc^{-1}). The angular correlation function is related to the spatial correlation function by an integral equation (see, for example, Peebles 1980). Parameterizing the evolution of $\xi(r)$ by

$$\xi(r,z) = \left(\frac{r}{r_0}\right)^{-\gamma} (1+z)^{-(3+\epsilon)}\,, \tag{6}$$

the relation between $\omega(\theta)$ and $\xi(r,z)$ for small angles is

$$\omega(\theta) = \sqrt{\pi}\frac{\Gamma[(\gamma-1)/2]}{\Gamma(\gamma/2)}\frac{A}{\theta^{\gamma-1}}r_0^{\gamma} \tag{7}$$

where

$$A = \int_0^\infty g(z)\left(\frac{dN}{dz}\right)^2 dz \left[\int_0^\infty \left(\frac{dN}{dz}\right) dz\right]^{-2}$$

and

$$g(z) = \left(\frac{dz}{dx}\right) x^{1-\gamma} F(x)\,(1+z)^{-(3+\epsilon-\gamma)}\,.$$

Here x is the coordinate distance at redshift z, r is the proper coordinate, dN/dz is the number of galaxies per unit redshift, and the metric is

$$ds^2 = c^2dt^2 - a^2[dx^2/F(x)^2 + x^2d\theta^2 + x^2\sin^2\theta d\phi^2].$$

For a power law parameterisation with constant γ, the evolution of $\xi(r)$ with redshift is given by ϵ. Assuming $\gamma = 1.8$, linear theory predicts $\epsilon = 0.8$, while clustering fixed in proper coordinates yields $\epsilon = 0.0$, and clustering fixed in comoving coordinates yields $\epsilon = -1.2$.

The small-scale clustering of galaxies is a highly non-linear process, and it is not at all obvious what value of ϵ to choose in order to compare model predictions of $\omega(\theta)$ to observations. Neither is it apparent that the assumption of a unique power law form for $\xi(r,z)$ is appropriate. Relatively few numerical studies of the evolution of $\xi(r)$ from redshifts of order $z \sim 3$–4 to the present have been performed. Yoshii, Peterson, & Takahara (1993) investigated the evolution of $\xi(r)$ of "density peak tracers" in N-body simulations of cold dark matter (CDM) universes from $z = 2$ to $z = 0$ and concluded that a flat CDM model is in agreement with the low clustering amplitude of faint galaxies observed by EBKTG.

Brainerd & Villumsen (1994) used a large N-body simulation to investigate the evolution of $\xi(r)$ of individual "dark matter halos" in a flat CDM universe from $z = 5$ to $z = 0$ and found that the evolution of $\xi(r)$ for these objects depended strongly on the parameters used to classify groups of particles as "halos" (eg. mass and overdensity). The correlation functions of moderate overdensity halos ($\delta\rho/\rho \sim 250$) and high-mass, high-overdensity halos ($\delta\rho/\rho \sim 2000$) were well-described by a power law whose index, γ, remained constant over the course of the simulation. However, γ for low-mass, high-overdensity halos increased continuously. In all cases, the "first generation" of halos was highly clustered, in agreement with the predictions of biased galaxy formation (eg. Bardeen *et al.* 1986). Over the epoch of halo formation, however, the distribution of moderate overdensity halos became *less* clustered than that of the first generation, while the very overdense halos remained at the same clustering strength. For those halos whose $\xi(r)$ was well described by a unique γ, two general patterns in the evolution of $\xi(r)$ were observed after all halos had

formed: $\epsilon = 0.0 \pm 0.2$ (low-mass, moderate-overdensity halos) and $\epsilon = -1.2$ (high-mass, moderate overdensity halos and high-mass, high-overdensity halos). In the following analysis we adopt these values of ϵ, along with the linear theory prediction $\epsilon = 0.8$, as representative of likely evolution in $\xi(r)$. We do note, however, that more rapid rates of clustering evolution have been observed in N-body simulations (eg. Melott 1992, Davis *et al.* 1985).

4 RESULTS AND DISCUSSION

Figure 1 shows $\hat{\omega}(\theta)$ for our three faintest samples together with the best-fit power laws, $A_\omega \theta^{-\delta}$, all of which have indices of $\delta \sim 0.8$. This indicates that the $\theta^{-0.8}$ power law form for $\hat{\omega}(\theta)$ measured at bright magnitudes continues all the way to our faintest sample. As observed by previous investigators, the amplitude of $\hat{\omega}(\theta)$ decreases with the effective depth of the catalogue. We illustrate this with Figure 2, in which we have plotted $\hat{\omega}(\theta)$ extrapolated to $\theta = 1^\circ$ (using $\hat{\omega}(\theta) \propto \theta^{-0.8}$) as a function of limiting R magnitude for a number of red-selected samples. It is readily apparent that our results extend the trend of weaker correlation at fainter depths, with no indication of any flattening of this decline to our faintest limits. A weighted linear least squares fit to the data in Figure 2 yields $\hat{\omega}(\theta = 1^\circ) \propto R^{-0.27 \pm 0.01}$. While these results are from only a single field, they are in qualitative agreement with preliminary results from a larger study by Bernstein & collaborators (Bernstein, priv. comm.).

The distribution of object colours on our frame radically changes at $r \sim 23$, when the median colour shifts from $g-r \sim 1$ to $g-r \sim 0.1$–0.2. Using these $g-r$ colours we, therefore, split the sample by colour at $g-r = 0.3$ and determine the relative clustering strengths of the "red" and "blue" galaxies. To within the measurement errors, there is no apparent difference in $\hat{\omega}(\theta)$ between the two subsamples.

We compare our observed amplitudes of $\hat{\omega}(\theta)$ with that predicted by our standard model, a single population of galaxies which have a present-day correlation length typical of local bright galaxy samples. For simplicity this population is assumed to have the same mix of galaxy types visible at each epoch. To make this comparison we calculate the appropriate NE $N(z)$ for a surface brightness selected sample of galaxies in each of our magnitude intervals (King & Ellis 1985) and, for convenience, we parameterise the shape of these predicted redshift distributions by (EBKTG)

$$\frac{dN}{dz} \propto z^2 \exp\left[-\left(\frac{z}{z_0}\right)^\beta\right]. \tag{8}$$

(It should be noted that the predicted correlation amplitude is dependent upon only the shape of $N(z)$ and not its normalisation.) Adopting $\gamma = 1.8$, $r_0 = 5.5h^{-1}$ Mpc, and choosing a value of ϵ, we calculate A_ω for different magnitude ranges using equation (7) above. The model parameters z_0 and β are summarized in Table 2 for the cases of (1) a flat universe with $\Omega_0 = 1$ and (2) an open universe with $\Omega_0 = 0.2$.

Figure 3 shows our observed variation in $A_\omega^{\rm corr}$ with limiting magnitude and model predictions using $N(z)$ from Table 2 with the choices of $\epsilon = -1.2$, 0.0, 0.8 and $\Omega_0 = 1.0$, 0.2. These models predict an amplitude that is about an order of magnitude greater than that observed. Clearly at least one of the assumptions in the models is incorrect. We first investigate the individual variation in each of the main model parameters (ϵ, $N(z)$, and r_0) necessary to match our observations.

If we allow only ϵ to vary in the models, then we find it must be of order 6 or 7 for the predicted amplitude to match that observed ($\epsilon_{\rm stan}$ in Table 2), implying a very rapid evolution in the correlation function: $\xi(z) \sim (1+z)^{-7}$. Such extreme evolution in the clustering of the *entire* population would have been easily detected by Cole *et al.* (1994) and, so, we prefer to search for another explanation.

One possibility is to relax our limits on the redshift distributions. By distributing the galaxies over both a wider range of redshifts and out to higher redshifts, it is possible to weaken the predicted clustering amplitude substantially. Using the measured correlation amplitude and assuming $\epsilon = 0.8$, we determine the minimum values of z_0 and β that are consistent with the 95% confidence level upper limit on the measured amplitude. This choice of ϵ allows for clustering that evolves at the rate predicted by linear theory and, amongst our 3 standard choices for ϵ, yields the lowest amplitude. To further constrain the possible distributions, in particular the value of β, we require that $N(z)$ comply with the limits on the fraction of galaxies with $z > 3$ from the study of Guhathakurta, Tyson & Majewski (1990). The minimum allowable parameters of the model $N(z)$ are given in Table 3 and indicate that by putting the galaxies at a higher median redshift, the growth of $\xi(r)$ required to match our observed amplitude of $\hat{\omega}(\theta)$ is much less extreme than that predicted using the $N(z)$ suggested by the lensing studies. However, to achieve the necessary dilution of the clustering strength we require the median redshifts in our sample to be roughly 3–4 times the values obtained from the lensing analyses. This seems unlikely, although such a distribution might be compatible if the scale sizes of faint galaxies decrease very strongly with redshift.

In our standard model we made the simplifying assumption that at each epoch we would observe the same mix of morphological types. This is not valid in our passband at the depths probed, even for the NE model. The 4000 Å break moves through the r-band at a redshift of $z \sim 0.7$, and this is the median redshift proposed for our faintest samples. The presence of strong 4000 Å breaks in early-type galaxies compared to late-types, in the absence of luminosity evolution, causes our deepest samples to be dominated by late-type spiral and irregular galaxies. At $r \sim 20$ the mix of types in the NE model is (E/S0/Sab, Sbc/Scd/Sdm): (98%, 2%). However, by $r \sim 26$ this has changed to (37%, 63%). In the Burst model this shift is even more extreme, as the 'excess' population in the faint counts consists exclusively of bursting gas-rich late-type spirals. This preeminence of moderate-redshift late-type systems in our catalogue is supported by the observed colour distribution, which peaks at $g-r \sim 0.1$–0.2, typical of late-type spirals and irregulars at $z \sim 1$. If these late-type galaxies are significantly less clustered than our adopted local sample, we would observe an amplitude for the correlation function which gradually falls below the predictions of our standard model at fainter magnitudes.

There exist local late-type galaxy populations that exhibit weaker clustering than the bright optical galaxy samples used in this comparison (e.g. dwarf galaxies, LSB galaxies, IRAS galaxies). These could serve as a natural mechanism for diluting the clustering strength of the faint galaxy samples through a progressive domination by weakly clustered, late-type dwarf galaxies. We can predict the necessary correlation length of these galaxies must have to agree with our observations. Summarised in Table 4 are the correlation lengths, r_0, required of this population in order to match the 95% confidence upper limits on our observed amplitudes. The choice of an open or closed universe makes little difference in the required correlation length, and for all three values of ϵ, r_0 is less than half the present-day correlation length of bright, optically-selected galaxies.

By a similar argument Bernstein *et al.* (1994) were able to construct a viable model for their observations by adopting the correlation function of IRAS galaxies for the dominant blue population in their $B \sim 22$ sample. They then required only modest clustering evolution ($\epsilon \sim 0$) for the bulk of their $z \sim 0.3$ population. Shown in Table 2 is the clustering evolution needed to reproduce our values of A_ω using a population described by the IRAS correlation function of SRRL ($\gamma \sim -1.6$ and $r_0 \sim 3.8h^{-1}$ Mpc). Under these assumptions our correlation function has to evolve as $\epsilon_{\rm IRAS} \sim 3$, which is slower than our standard model predicts, but considerably faster than the theoretical predictions.

We would claim that the IRAS correlation function is probably not the correct choice to describe the faint galaxy population. A more representative local sample would be either dwarf or

LSB galaxies (see McGaugh 1994), especially within the framework of the Burst model described above. Two recent, large studies have measured correlation functions for similar classes of galaxies. Santiago & da Costa (1990) used volume-limited samples from the new Southern Sky Redshift Survey (SSRS) to study the clustering of LSBs, while Thuan *et al.* (1991) analysed a mixed sample of dwarf and LSB galaxies from the UGC. The more interesting of these is the SSRS study which finds a correlation length for LSB galaxies of $r_0 \sim 2.3$–$2.7h^{-1}$ Mpc, depending upon the exact sample definition. These local values are somewhat uncertain due to the small samples available, however, the range of values is in reasonable agreement with those quoted in Table 4 for clustering growth of $\epsilon \sim 0.8$. It therefore appears that we can achieve a sufficiently low amplitude for $\omega(\theta)$ at faint limits by postulating a gradual transition to LSB, late-type dominated samples via differential K-corrections, coupled with the intrinsically weaker clustering of these galaxies.

5 CONCLUSIONS

We have measured the angular correlation function of galaxies to an apparent magnitude limit of $r \leq 26$. The correlation amplitude, A_ω, for our faintest sample is extremely small, but significantly non-zero. This detection is approximately an order of magnitude weaker than the predictions of a theoretically and observationally motivated standard model. The amplitude of the correlation function decreases continuously to our faintest limits, showing no evidence for any flattening (c.f. RSMF). We find no difference between the clustering strength of the blue and red galaxies within our sample.

There are three main parameters in our standard model which can be varied in order to obtain agreement with the observations: the evolution in $\xi(r)$ (parameterised by ϵ), the redshift distribution of the sample, $N(z)$, and the correlation length, r_0. Forcing the observed low correlation amplitude to result from a variation of either ϵ or $N(z)$ results in two unpalatable solutions: extremely rapid (and unexpected) evolution in $\xi(r)$ or a redshift distribution in which the galaxies are distributed at median redshifts 3–4 times that expected from gravitational lensing studies of rich clusters.

We prefer a more natural explanation for the low clustering strength observed, resulting from the tendency of deep field samples to be dominated by moderate-redshift, blue star-forming spiral and irregular galaxies. This arises from the different K-corrections for early- and late-type systems. However, this effect is magnified by the overwhelming prevalence of blue late-type systems in faint field counts, as illustrated by the trend to bluer colours at fainter magnitudes. In the Burst model of Broadhurst, Ellis & Shanks (1990) these late-type systems are associated with star bursting LSB and dwarf galaxies. Assuming modest clustering growth we derive a correlation length for these late-type systems of $r_0 \sim 2h^{-1}$ Mpc. This is significantly shorter than the equivalent value for either local bright optically-selected galaxies, or IRAS-selected galaxies. However, it is in reasonable agreement with the correlation lengths measured for LSB galaxies from the recent SRSS (Santiago & da Costa 1990).

We find reasonable support for a simple model of faint galaxy evolution where luminous galaxies are distributed out to modest redshifts ($z \sim 1$) and the high galaxy surface density is made up of a dominant co-eval population of bursting LSB galaxies. The clustering of this dominant, bursting population can be explained by plausible theoretical clustering evolution of the locally observed samples.

A simple observational test of our model for the clustering of faint galaxies would be a correlation analysis of a deep infra-red (K) selected sample, which should show significantly stronger clustering than we observe. This results from the dominance, out to high redshifts, of the same early-type galaxies which define the local bright optically-selected samples.

ACKNOWLEDGEMENTS

We acknowledge useful conversations with Gary Bernstein, Roger Blandford, Warrick Couch, and Raja Guhathakurta. We thank Alan Dressler for leading the construction of the COSMIC instrument. Support under NSF grants AST-89-17765 (TGB) and a NATO Postdoctoral Fellowship (IRS) is gratefully acknowledged.

REFERENCES

Babul, A. & Rees, M.J., 1992, MNRAS, 255, 346.
Bahcall, J.N. & Soneira, R.M., 1980, ApJS, 47, 357.
Bardeen, J. M., Bond, J. R., Kaiser, N., & Szalay, A. S. 1986, ApJ, 304, 15
Barrow, J.D., Bhavsar S.P. & Sonoda, D.H., 1984, MNRAS, 210, 19.
Bernstein, G.M., Tyson, J.A., Brown, W.R. & Jarvis, J.F., 1994, ApJ, 426, 516.
Brainerd, T.G. & Villumsen, J.V., 1994, ApJ, in press.
Broadhurst, T.J., Ellis, R.S. & Shanks, T., 1988, MNRAS, 235, 827.
Broadhurst, T.J., Ellis, R.S. & Glazebrook, K., 1992, Nature, 355, 55.
Cole, S., Ellis, R., Broadhurst, T. & Colless, M., 1994, MNRAS, 267, 541.
Couch, W.J., Jurcevic, J.S. & Boyle, B.J., 1993, MNRAS, 260, 241 (CJB).
Davis, M., Efstathiou, G., Frenk, C. S., & White, S. D. M. 1985, ApJ, 292, 371
Efstathiou, G., Bernstein, G., Katz, N., Tyson, J.A. & Guhathakurta, P., 1991, ApJ, 380, L47 (EBKTG).
Fisher, K.B., Davis, M., Strauss, M.A., Yahil, A. & Huchra, J., 1994, MNRAS, 266, 50.
Glazebrook, K., Ellis, R.S., Colless, M., Broadhurst, T.J., Allington-Smith, J., Tanvir, N. & Taylor, K. 1994 MNRAS, in press.
Groth, E.J. & Peebles, P.J.E., 1977, ApJ, 217, 385.
Kent, S.M., 1985, PASP, 97, 165.
King, C.R. & Ellis. R.S., 1985, ApJ, 288, 456.
Kneib, J.-P., Mathez, G., Fort, B., Mellier, Y., Soucail, G. & Langaretti, P.-Y., 1994, preprint.
Koo, D.C. & Szalay, A.S., 1984, ApJ, 282, 390.
Landy, S.D. & Szalay, A.S., 1993, ApJ, 412, 64.
Lilly, S.J., Cowie, L.L. & Gardner, J.P., 1991, ApJ, 369, 79.
Maddox, S.J., Sutherland, W.J., Efstathiou, G., Loveday, J., 1990, MNRAS, 234, 692.
McGaugh, S.S., 1994, Nature, 367, 538.
Melott, A. 1992, ApJ, 393, L45
Mould, J.R., Blandford, R.D., Villumsen, J.V., Brainerd, T.G., Smail, I., Small, T.A. & Kells, W., 1994, MNRAS, submitted.
Neuschaefer, L.W., Windhorst, R.A. & Dressler, A., 1991, ApJ, 382, 32 (NWD).
Peebles, P.J.E., 1980, 'The Large-Scale of the Universe', Princeton Univ. Press.
Guhathakurta, P., Tyson, J.A. & Majewski, S.R., 1990, ApJ, 357, L9.
Roche, N., Shanks, T., Metcalfe, N. & Fong, R., 1993, MNRAS, 263, 360 (RSMF).
Santiago, B.X. & da Costa, L.N., 1990, 362, 386.
Saunders, W., Rowan-Robinson, M. & Lawrence, A., 1992, MNRAS, 258, 134 (SRRL).
Shanks, T., Fong, R., Ellis, R.S. & MacGillivray, H.T., 1980, 192, 209.
Soneira, R.M. & Peebles, P.J.E., 1978, AJ, 83, 845.
Stevenson, P.R., Shanks, T., Fong, R. & MacGillivray, H.T., 1985, MNRAS, 213, 953 (SSFM).
Smail, I., Ellis, R.S., Aragòn-Salamanca, A., Soucail, G., Mellier, Y. & Giraud, E. 1993, MNRAS, 263, 628.

Smail, I., Ellis, R.S. & Fitchett, M.J., 1994, MNRAS, in press.
Valdes, F. 1982, FOCAS Manual, NOAO.
Yoshii, Y., Peterson, B.A. & Takahara, F., 1993, ApJ, 414, 431.

FIGURES

Figure 1: The two-point angular correlation function of galaxies in 3 magnitude intervals: (a) $20.0 \leq r \leq 25.0$, (b) $20.0 \leq r \leq 25.5$, (c) $20.0 \leq r \leq 26.0$). No correction for the integral constraint has been made. Error bars are estimated from 50 bootstrap resamplings of the data. The best-fit power laws of the form $\omega(\theta) = A\theta^{-0.8}$ are indicated by the dotted lines. Note that different vertical scales are used in each panel.

Figure 2: Corrected $\hat{\omega}(\theta)$ extrapolated 1 degree as function of limiting R magnitude for a number of red selected samples. The magnitude limits for the CJB study have been converted to R using the transformations given by Yoshii, Peterson & Takahara (1993) and RSMF. This figure is adapted from Roche *et al.* (1993).

Figure 3: Observed correlation function amplitude, $A_\omega^{\rm corr}$, as a function of limiting r magnitude (squares). Error bars indicate 95% confidence limits. The predicted amplitude as a function of limiting magnitude, ϵ, and Ω_0 (assuming $r_0 = 5.5h^{-1}$ Mpc and $\gamma = 1.8$) is indicated by lines (solid for $\Omega_0 = 1.0$; dashed for $\Omega_0 = 0.2$). Also shown (dotted line) is the predicted $A_\omega^{\rm corr}$ assuming $r_0 = 2.0h^{-1}$ Mpc, $\Omega_0 = 1.0$, $\gamma = 1.8$, and $\epsilon = 0.8$.

Table 1: Observed correlation function parameters

mag. interval	$N_{\rm obs}$	$\left(\frac{N_{\rm obs}}{N_{\rm obs}-N_{\rm s}}\right)^2$	$A_\omega^{\rm corr}$	$\hat{\omega}(\theta=1^\circ)$
$20.0 \le r \le 24.5$	2170	1.439	0.37±0.04	$(5.3 \pm 0.6) \times 10^{-4}$
$20.0 \le r \le 25.0$	3103	1.329	0.31±0.04	$(4.4 \pm 0.6) \times 10^{-4}$
$20.0 \le r \le 25.5$	4292	1.258	0.20±0.03	$(2.9 \pm 0.4) \times 10^{-4}$
$20.0 \le r \le 26.0$	5730	1.206	0.11±0.02	$(1.6 \pm 0.3) \times 10^{-4}$

Table 2: Parameters for $N(z)$ assuming a NE model and corresponding evolution of $\omega(\theta)$

	$\Omega_0 = 1.0$				$\Omega_0 = 0.2$			
mag. interval	z_0	β	$\epsilon_{\rm stan}$	$\epsilon_{\rm IRAS}$	z_0	β	$\epsilon_{\rm stan}$	$\epsilon_{\rm IRAS}$
$20.0 \le r \le 24.5$	0.49	2.5	7	3	0.45	2.4	7	3
$20.0 \le r \le 25.0$	0.58	2.7	6	3	0.48	2.4	7	3
$20.0 \le r \le 25.5$	0.65	2.7	6	3	0.55	2.5	7	3
$20.0 \le r \le 26.0$	0.75	2.8	7	4	0.64	2.7	7	4

Table 3: Shallowest $N(z)$ consistent with the 95% confidence level upper limit on $\hat{\omega}(\theta)$

	$\Omega_0 = 1.0$		$\Omega_0 = 0.2$	
mag. interval	z_0	β	z_0	β
$20.0 \le r \le 24.5$	1.4	3	1.4	6
$20.0 \le r \le 25.0$	1.8	4	1.6	6
$20.0 \le r \le 25.5$	2.4	6	1.8	6
$20.0 \le r \le 26.0$	—	–	2.5	6

Table 4: Correlation length, r_0 (h^{-1} Mpc), required to match $A_\omega^{\rm corr}$ assuming a NE model $N(z)$ and $\delta = 0.8$ (0.6)

	$\Omega_0 = 1.0$			$\Omega_0 = 0.2$		
mag. interval	$\epsilon = -1.2$	$\epsilon = 0.0$	$\epsilon = 0.8$	$\epsilon = -1.2$	$\epsilon = 0.0$	$\epsilon = 0.8$
$20.0 \le r \le 24.5$	1.4 (1.7)	1.8 (2.2)	2.1 (2.6)	1.5 (1.8)	1.9 (2.3)	2.2 (2.7)
$20.0 \le r \le 25.0$	1.4 (1.7)	1.8 (2.3)	2.2 (2.8)	1.5 (1.8)	1.8 (2.3)	2.2 (2.8)
$20.0 \le r \le 25.5$	1.2 (1.4)	1.6 (2.0)	2.0 (2.4)	1.3 (1.5)	1.7 (2.0)	2.0 (2.4)
$20.0 \le r \le 26.0$	0.9 (1.0)	1.3 (1.5)	1.6 (1.9)	1.0 (1.1)	1.3 (1.5)	1.6 (1.9)

Fig. 1

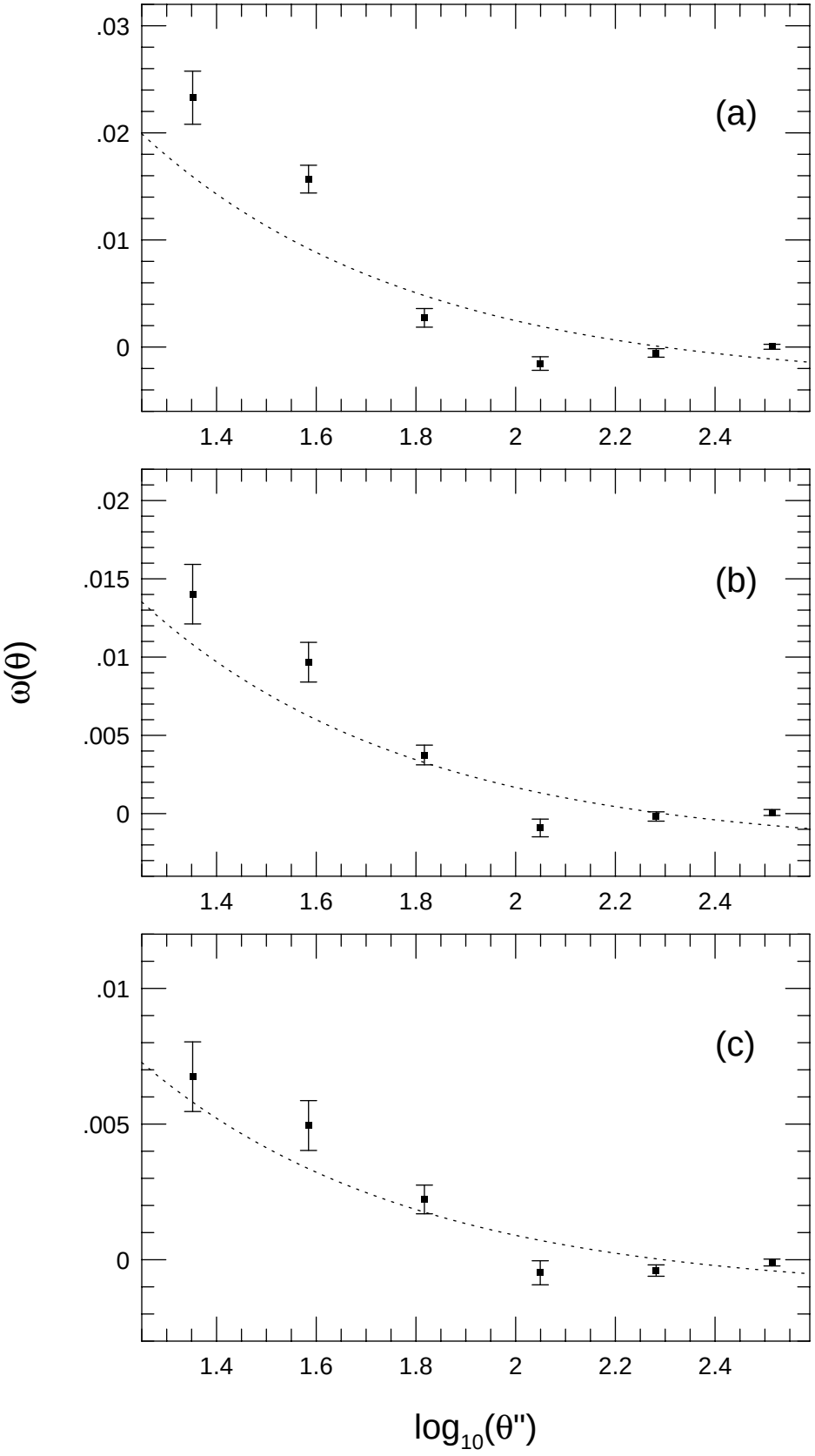

Fig. 2

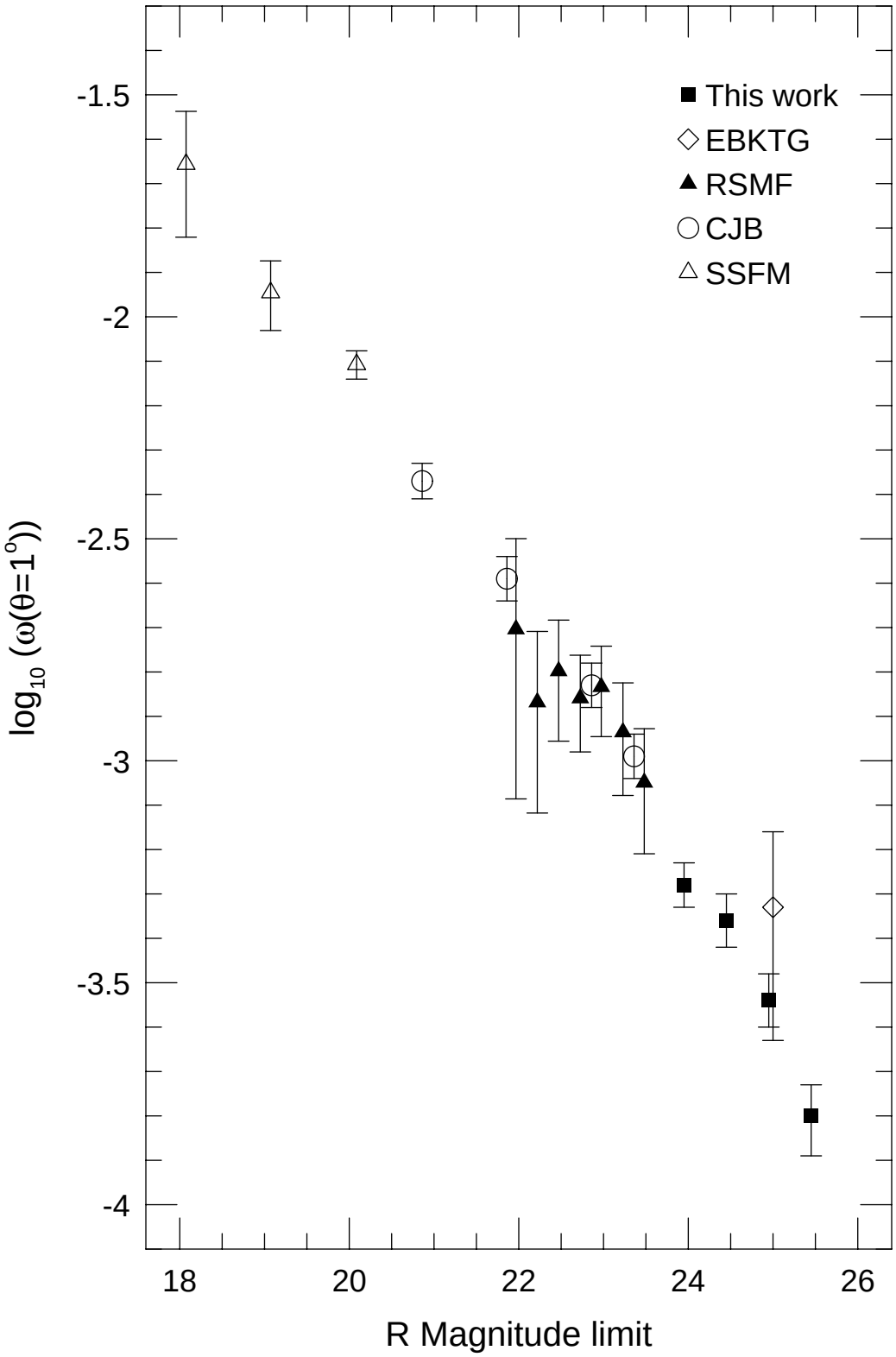
This work
EBKTG
RSMF
CJB
SSFM
-1.5
-2
-2.5
-3
-3.5
-4
18
20
22
24
26
log10 (ω(θ=1°))
R Magnitude limit

Fig. 3

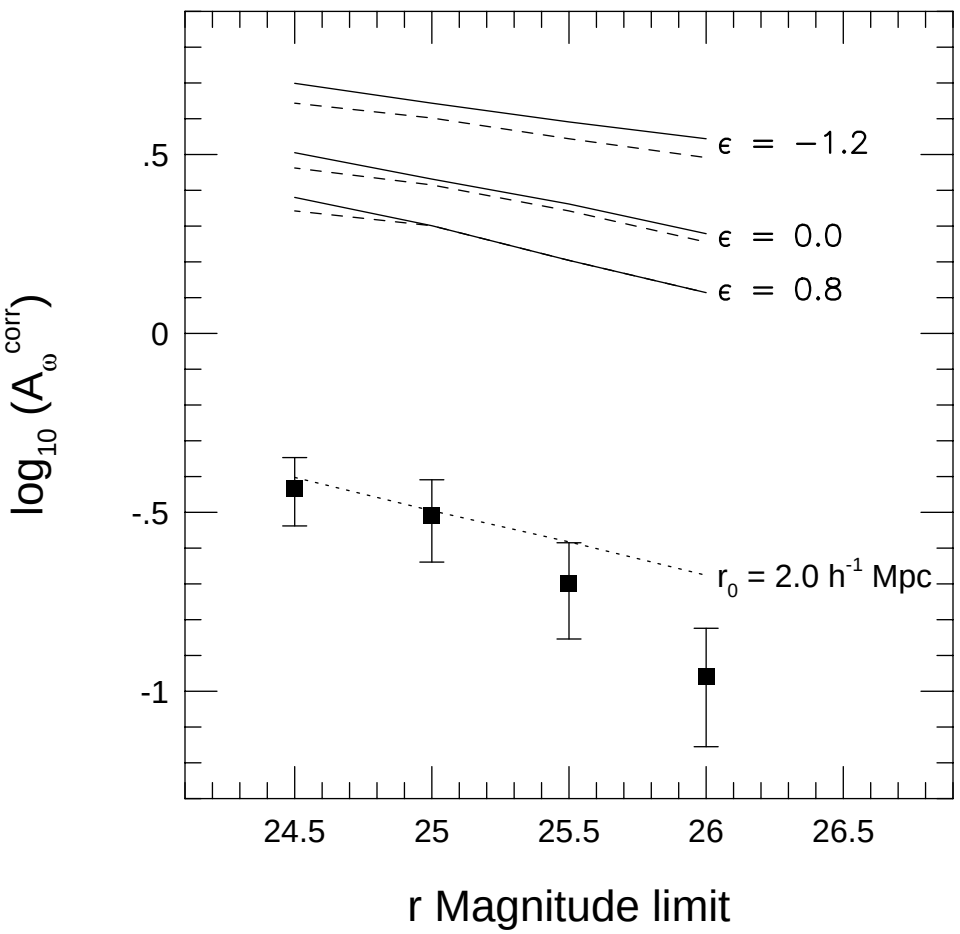
.5
0
-.5
-1
log10 (Aω corr)
ϵ = −1.2
ϵ = 0.0
ϵ = 0.8
r0 = 2.0 h-1 Mpc
24.5
25
25.5
26
26.5
r Magnitude limit